

# Switching performance of quasi-vertical GaN-based p-i-n diodes on Si

Xu Zhang<sup>1</sup>, Xinbo Zou<sup>1,2</sup>, Chak Wah Tang<sup>1</sup>, and Kei May Lau<sup>\*1,2</sup>

<sup>1</sup> Department of Electronic and Computer Engineering, Hong Kong University of Science and Technology, Clear Water Bay, Kowloon, Hong Kong

<sup>2</sup> HKUST Jockey Club Institute for Advanced Study (IAS), Hong Kong University of Science and Technology, Hong Kong

Received 30 October 2016, revised 19 April 2017, accepted 20 April 2017

Published online 17 May 2017

**Keywords** forward recovery, GaN silicon, PIN diodes, reverse recovery, switching

\* Corresponding author: e-mail eekmlau@ust.hk, Phone: +852 2358 7049, Fax: +852 2358 1485

The switching performance of GaN-based p-i-n diodes on Si was investigated for the first time. A double-pulse test circuit using an inductive load was utilized to evaluate the diode's switching characteristics. When the GaN diode was switched from an on-state with  $I_F = 450$  mA to an off-state with  $V_R = -200$  V ( $dI_F/dt = 16$  A/ $\mu$ s), the peak reverse recovery current ( $I_{rr}$ ) and time ( $t_{rr}$ ) was measured to be 19.4 mA and 7.1 ns, respectively. The amount of charges stored in the drift region and the turn-off energy was extracted to be 0.14 nC and 0.054  $\mu$ J, respectively. The carrier lifetime under high-level

injection conditions in GaN was estimated to be 0.6 ns. The reverse recovery characteristics of the GaN diodes showed little sensitivity to elevated temperatures up to 150 °C. During the forward recovery (from off-state with  $V_R = -190$  V to on-state with  $I_F = 450$  mA), the GaN diode exhibited a negligible voltage overshoot. In comparison to a commercial fast recovery-Si diode, the superior reverse and forward recovery performance of GaN-based p-i-n diodes indicates their practicality in fast switching applications and reliability at high temperatures.

© 2017 WILEY-VCH Verlag GmbH & Co. KGaA, Weinheim

**1 Introduction** III-N semiconductor materials have invigorated intensive research in various optoelectronic and electronic devices for the next generation solid-state lighting (SSL), high frequency and high power applications due to their superior material properties, such as wide energy bandgap, high critical electrical field and good thermal conductivity [1–3]. Along with the development of conventional lateral devices, such as AlGaIn/GaN high electron mobility transistors (HEMTs) [4, 5], vertically configured diodes and transistors [6, 7] have also been extensively investigated in recent years. The vertical structure enables high breakdown voltage with a small footprint, good thermal performance and high integration flexibility. As a fundamentally important and widely used device, GaN-based p-i-n diodes have also been investigated because of their small conduction loss, low reverse leakage current, and high breakdown voltage [8–12].

With continuous progress in growing GaN on (111)Si substrates, GaN on silicon electronics is considered an enabling technology capitalizing on the outstanding material properties of GaN and volume production offered by Si. Recently, a number of two-terminal devices

including GaN Schottky diode, quasi-vertical p-i-n diode, and fully-vertical p-i-n diode have been successfully demonstrated using GaN-on-Si epilayers [13–15]. The reported device technologies and diode characteristics showed a great potential of these devices in high voltage applications.

However, there is no report on the switching performance of p-i-n diodes using GaN-on-Si epilayers, which is important information especially for high-frequency switching applications. In this work, we demonstrated for the first time the switching performance of quasi-vertical p-i-n diodes grown and fabricated on (111)Si substrates. Both reverse and forward recovery characteristics of GaN-based p-i-n diodes are reported and discussed. A detailed comparison between a GaN diode and a commercial fast recovery-Si diode is also made.

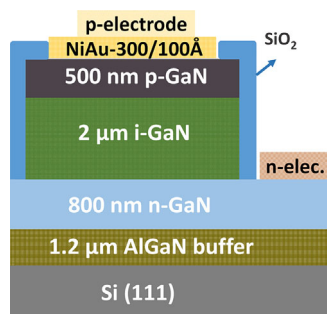
**2 Device information and measurement setup** The p-i-n diode structures were grown by metal-organic vapor phase epitaxy (MOVPE) on a 6-inch Si substrate. After depositing a 1.2- $\mu$ m thick AlGaIn buffer layer, a 800-nm thick Si-doped n-GaN layer ( $\sim n = 2 \times 10^{18}$  cm<sup>-3</sup>)

was grown, followed by a 2- $\mu\text{m}$ -thick undoped i-GaN drift layer and a 500-nm thick Mg-doped p-type GaN cap layer ( $\sim p = 2 \times 10^{17} \text{ cm}^{-3}$ ). In device fabrication, the n-GaN was first exposed using inductively coupled plasma (ICP) dry etching. To suppress leakage current through the etched sidewall, treatment in a 75 °C tetramethylammonium hydroxide (TMAH) to remove etching damage is carried out, and followed by sidewall passivation [16] by  $\text{SiO}_2$  using plasma enhanced chemical vapor deposition (PECVD). Then the metal stack with 30 nm/10 nm NiAu was deposited onto the p-GaN and annealed to form Ohmic contacts. Finally, Cr/Al-based metal were deposited as electrodes. The schematic of a completed device is shown in Fig. 1.

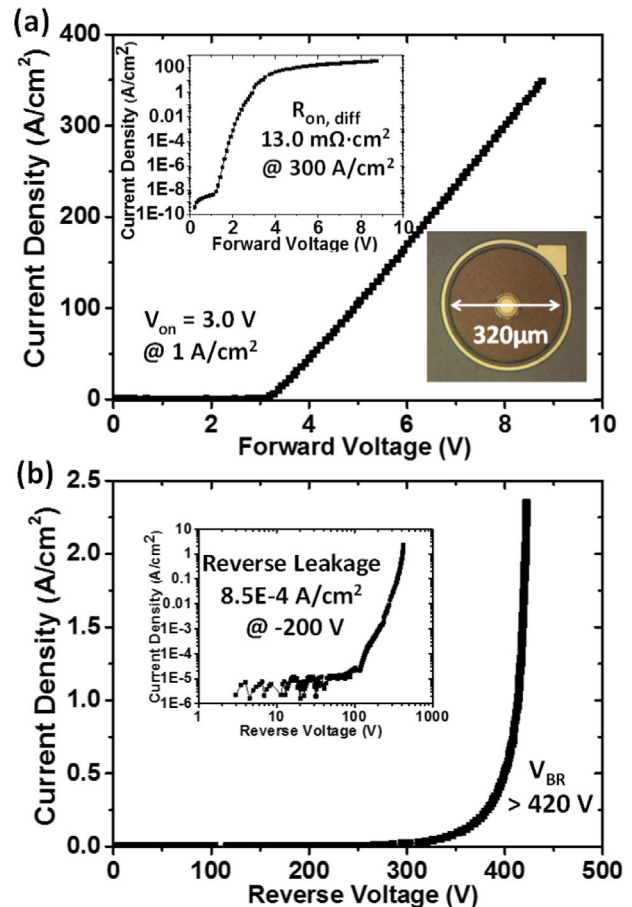
Figure 2(a) shows the forward  $I$ - $V$  characteristics of a  $0.08 \text{ mm}^2$  quasi-vertical p-i-n diode. The  $V_{\text{on}}$  can be extracted as 3.0 V at  $1 \text{ A cm}^{-2}$ . It was calculated that the differential  $R_{\text{on}}$  was  $13 \text{ m}\Omega\text{-cm}^2$  after turn on. The reverse  $I$ - $V$  characteristics (Fig. 2(b)), shows the leakage current density as low as  $8.5 \times 10^{-4} \text{ A cm}^{-2}$  at a bias of  $-200 \text{ V}$ . A sharp breakdown was observed at a reverse bias of 420 V, which is corresponding to a critical electrical field of  $2.1 \text{ MV cm}^{-1}$ .

Figure 3 is a double-pulse test circuit using an inductive load utilized to evaluate the diode's switching performance and energy loss [17]. A 1.7 kV commercial SiC MOSFET was employed to serve as a switch. When the first pulse signal was applied to the transistor, it is first turned on and the inductor (5 mH) is charged linearly by the DC power supply ( $V_{\text{DD}} = 200 \text{ V}$ ) while the device under test (DUT) is reverse-biased. Once the transistor is turned off, the inductor current would go through the DUT and driven into a forward-biased state. When the second pulse comes, the MOSFET will be switched on inducing the DUT to enter the reverse-blocking state again.

**3 Switching performance** During the on-state of the GaN diode with high current density, there is a large amount of free carriers being injected into the drift region. To enter the off-state, these carriers must be totally removed before a depletion region can be established to support the reverse bias blocking function. As the diode is being switched from the on-state to off-state, a peak reverse



**Figure 1** Schematic of Quasi-vertical GaN-based p-i-n diodes.



**Figure 2** (a) Forward and (b) Reverse  $I$ - $V$  characteristics of GaN-based quasi-vertical p-i-n diodes. Inset of (a) is an optical image of a circular diode with a diameter of  $320 \mu\text{m}$ .

recovery current ( $I_{\text{rr}}$ ) will occur during the removal of the stored charges in the drift region.

Figure 4 compares the reverse recovery characteristics of the GaN-on-Si and Si diodes (Fairchild, UF4004) when being switched from a forward current of 450 mA to a reverse-blocking mode ( $V_{\text{R}} = -200 \text{ V}$ ) with a fixed differential of  $dI_{\text{F}}/dt = 16 \text{ A } \mu\text{s}^{-1}$ . Compared to the Si diodes, the GaN diodes exhibited a  $30\times$  reduction in peak reverse recovery current ( $\sim 19.4 \text{ mA}$ ) and a  $9\times$  reduction in reverse recovery time ( $t_{\text{rr}}$ ,  $\sim 7 \text{ ns}$ ). This is mainly attributed to the much shorter carrier lifetime in GaN so

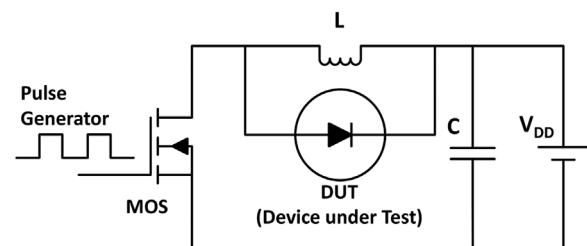


**Figure 3** Schematic of double-pulse test circuit.

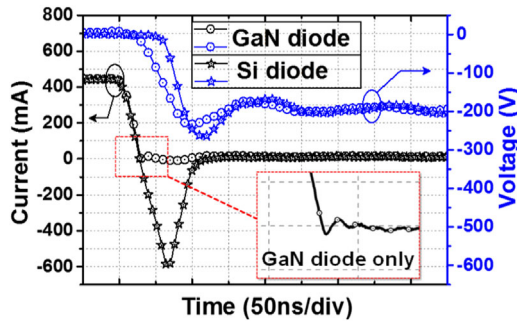


**Figure 4** Voltage and current waveforms of GaN-based quasi-vertical diode and fast Si diode (Fairchild, UF4004) during reverse recovery. The inset is a zoomed-in image at the point where the GaN diode's peak reverse recovery current occurs.

that the charges in the drift layer can be removed within a much short time frame. From the reverse recovery characteristics, the carrier lifetime of p-i-n diode in high-level injection conditions ( $\tau_{HL}$ ) can be calculated as [18]

$$\tau_{HL} = 2 \times \frac{I_{rr}}{I_F} \times t_{rr}, \quad (1)$$

where the  $I_F$  is the forward current. Correspondingly, the carrier lifetime under high-level injection conditions in GaN p-i-n diodes can be estimated as 0.6 ns compared to that of 170 ns for Si diodes.

As summarized in Table 1, the estimated charges stored in the drift region of the GaN diodes is 0.14 nC, only around 0.6% of that in Si diodes. The much smaller amount of charges stored in the GaN diodes are directly related to the thin drift layer (2  $\mu\text{m}$  thick) and small device area. As a result, the turn-off energy of GaN diode for one reverse recovery event can be calculated to be 0.054  $\mu\text{J}$ , which was only 2.5% of that in a Si diode (2.14  $\mu\text{J}$ ).

Figure 5(a) shows the reverse recovery characteristics from different forward currents to the same reverse-blocking mode ( $V_R = -200\text{ V}$ ). The larger the forward current, the larger amount of charges will be injected into the drift region prolonging the reverse recovery

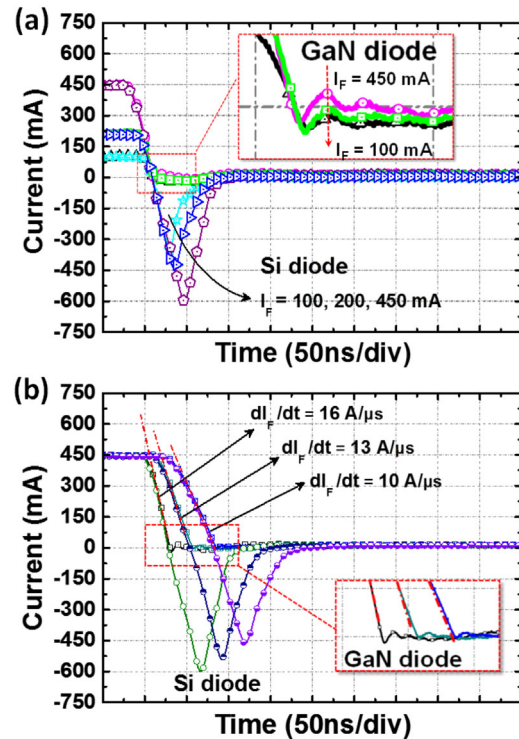


**Figure 5** Current waveforms of the two diodes during reverse recovery (a) from different forward currents to reverse-blocking state ( $V_R = -200\text{ V}$ ) and (b) from forward current of 450 mA to reverse-blocking state ( $V_R = -200\text{ V}$ ) under different current change rate. The insets are zoomed-in images at the point where the GaN diode's peak reverse recovery current occurs.

process. For the Si diode, both of  $I_{rr}$  and  $t_{rr}$  increase significantly as the forward current rises from 100 to 200 mA, and then 450 mA. Meanwhile, less impact was observed for the GaN diode. Figure 5(b) presents the influence of  $dI_F/dt$  on reverse recovery. If the  $dI_F/dt$  is smaller, the forward current will drop slower to zero during which less charges will be left for the reverse recovery process. With decreasing  $dI_F/dt$ , the Si diode only exhibited slightly suppressed reverse recovery current and time which, however, are still much larger than that in the GaN diode.

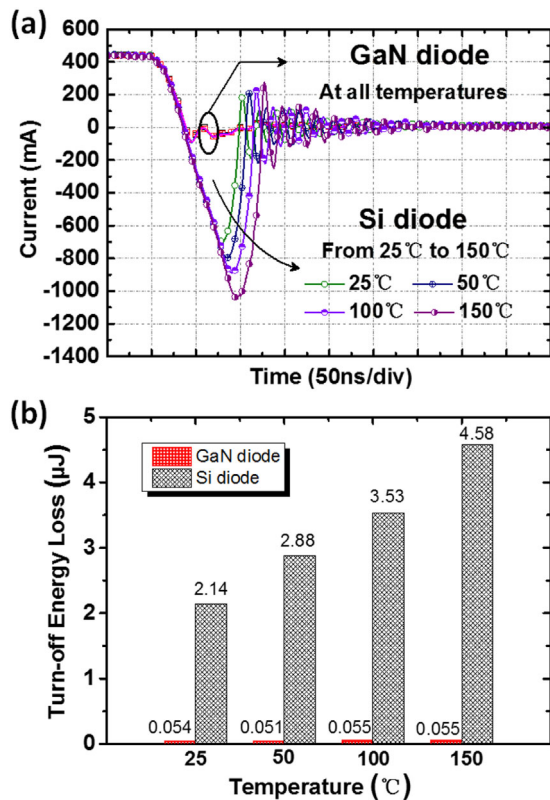
Figure 6 displays reverse recovery characteristics of GaN diodes and Si diodes at different temperatures. As temperatures rise from 25 to 150  $^{\circ}\text{C}$ , the peak reverse recovery current for the Si diodes increased to 1 A and the reverse recovery time was as large as 187 ns. While little influence has been observed for GaN p-i-n diodes up to 150  $^{\circ}\text{C}$ . As a result, a turning-off energy loss was calculated to be 4.58  $\mu\text{J}$  at 150  $^{\circ}\text{C}$  for Si diodes (over two times larger than that at 25  $^{\circ}\text{C}$ ) [Fig. 6(b)]. While the turning-off energy loss of GaN diodes show excellent thermal immunity for temperatures up to 150  $^{\circ}\text{C}$  due to the wide energy bandgap of GaN material (3.4 eV).

Figure 7 displays the forward recovery characteristic of a GaN-based quasi-vertical p-i-n diode compared to the fast

**Table 1** Summary of the parameters during reverse recovery.

parameter	GaN diode	Si diode
$I_{rr}$ (mA)	19.4	598.3
$t_{rr}$ (ns)	7.1	64.1
$Q_{rr}$ (nC)	0.14	23.67
$\tau_{HL}$ (ns)	0.6	170
turn-off energy ( $\mu\text{J}$ )	0.054	2.14

\*Parameters during reverse recovery of GaN-based quasi-vertical diode and fast Si diode (Fairchild, UF4004), from a forward current of 450 mA to a reverse-blocking mode ( $V_R = -200\text{ V}$ ). ( $t_{rr}$  was defined as the time duration from the point where the forward current drops to zero to the point where the reverse recovery current decays to 20% of  $I_{rr}$ ).



**Figure 6** (a) Reverse recovery characteristics at different temperatures. (b) Turn-off energy loss of the two diodes at different temperatures.

Si diode. When switched from a reverse blocking mode ( $V_R = -190\text{ V}$ ) to a forward conduction mode with current of 450 mA, the peak of the voltage overshoot reached around 20 V for the Si diode while no obvious voltage overshoot was observed for the GaN diode. As the overshoot voltage is largely related to the highly-resistive unmodulated portion of the drift layer, an overshoot voltage is expected in the Si diode due to the large and thick active area. In contrast, the GaN diode benefits from its thin drift layer (only 2  $\mu\text{m}$  thick) that only a small number of charge is needed to finish the OFF-to-ON transient and thus, a

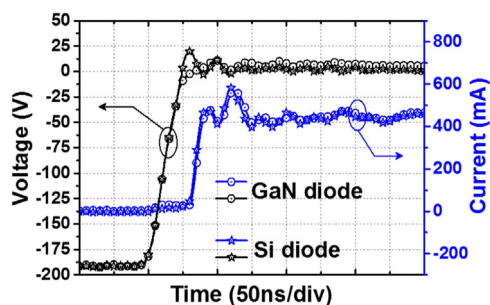


**Figure 7** Voltage and current waveforms of the two diodes during forward recovery.

negligible voltage overshoot was observed. As a result, a much smaller energy loss during forward recovery could be expected from the GaN diodes.

**4 Conclusions** The switching performance was demonstrated for GaN-based p-i-n diodes on Si. During reverse recovery (from on-state with  $I_F = 450\text{ mA}$  to off-state with  $V_R = -200\text{ V}$ ,  $dI_F/dt = 16\text{ A}\mu\text{s}^{-1}$ ), the GaN diode exhibited superior performance to Si diodes, including a peak reverse recovery current of only 19.4 mA, reverse recovery time of 7.1 ns, stored charge of 0.14 nC, and turn-off energy of 0.054  $\mu\text{J}$ . The reverse recovery characteristics of the GaN diodes showed very good temperature immunity for temperatures up to 150  $^{\circ}\text{C}$ , which indicated their practical application at high temperature harsh environment. During the forward recovery (from off-state with  $V_R = -190\text{ V}$  to on-state with  $I_F = 450\text{ mA}$ ), the GaN diode presented negligible voltage overshoot compared to a 20 V overshoot voltage peak observed in the commercial fast recovery-Si diode. The reverse and forward recovery characteristics of p-i-n diodes using GaN-on-Si epilayers show great promise in high frequency switching applications.

**Acknowledgements** This work was supported by the Research Grants Council (RGC) theme-based research scheme (TRS) of the Hong Kong Special Administrative Region Government under grant T23-612/12-R, and partially supported by a grant from the Research Grants Council of the Hong Kong Special Administrative Region (Project No. 16213915).

## References

- [1] S. J. Pearton and F. Ren, *Adv. Mater.* **12**(21), 1571 (2000).
- [2] M. S. Shur, *Solid-State Electron.* **42**(12), 2131 (1998).
- [3] N. Ikeda, Y. Niiyama, H. Kambayashi, Y. Sato, T. Nomura, S. Kato, and S. Yoshida, *Proc. IEEE* **98**(7), 1151 (2010).
- [4] Y. F. Wu, A. Saxler, M. Moore, R. P. Smith, S. Sheppard, P. M. Chavarkar, T. Wisleder, U. K. Mishra, and P. Parikh, *IEEE Electron. Device Lett.* **25**(3), 117 (2004).
- [5] W. Saito, Y. Takada, M. Kuraguchi, K. Tsuda, I. Omura, T. Ogura, and H. Ohashi, *IEEE Trans. Electron. Devices* **50**(12), 2528 (2003).
- [6] H. Nie, Q. Diduck, B. Alvarez, A. P. Edwards, B. M. Kayes, M. Zhang, G. Ye, T. Prunty, D. Bour, and I. C. Kizilyalli, *IEEE Electron. Device Lett.* **35**(9), 939 (2014).
- [7] S. Chowdhury, B. L. Swenson, M. H. Wong, and U. K. Mishra, *Semicond. Sci. Technol.* **28**(7), 074014 (2013).
- [8] Y. Hatakeyama, K. Nomoto, A. Terano, N. Kaneda, T. Tsuchiya, T. Mishima, and T. Nakamura, *Jpn. J. Appl. Phys.* **52**(2), 028007 (2013).
- [9] T. G. Zhu, D. J. H. Lambert, B. S. Shelton, M. M. Wong, U. Chowdhury, H. K. Kwon, and R. D. Dupuis, *Electron. Lett.* **36**(23), 1971 (2000).
- [10] Y. Yoshizumi, S. Hashimoto, T. Tanabe, and M. Kiyama, *J. Cryst. Growth* **298**(SPEC. ISS), 875 (2007).

- [11] I. C. Kizilyalli, A. P. Edwards, H. Nie, D. Disney, and D. Bour, *IEEE Trans. Electron. Devices* **60**(10), 3067 (2013).
- [12] I. C. Kizilyalli, T. Prunty, and O. Aktas, *IEEE Electron. Device Lett.* **36**(10), 1073 (2015).
- [13] X. Zou, X. Zhang, X. Lu, C. W. Tang, and K. M. Lau, *IEEE Electron Device Lett.* **37**(5), 636 (2016).
- [14] Y. Zhang, M. Sun, D. Piedra, M. Azize, X. Zhang, T. Fujishima, and T. Palacios, *IEEE Electron. Device Lett.* **35**(6), 618 (2014).
- [15] X. Zou, X. Zhang, X. Lu, C. W. Tang, and K. M. Lau, *IEEE Electron. Device Lett.* **37**(9), 1158 (2016).
- [16] Y. Zhang, M. Sun, H. Y. Wong, Y. Lin, P. Srivastava, C. Hatem, M. Azize, D. Piedra, L. Yu, T. Sumitomo, N. De Almeida Braga, R. V. Mickevicius, and T. Palacios, *IEEE Trans. Electron. Devices* **62**(7), 2155 (2015).
- [17] B. Ozpineci and L. M. Tolbert, *IEEE Power Electron. Lett.* **1**(2), 54 (2003).
- [18] B. J. Baliga, *Fundamentals of Power Semiconductor Devices* (Springer, US, 2010).